Control Engineering Practice 36 (2015) 133–141

Contents lists available at ScienceDirect

Control Engineering Practice

journal homepage: www.elsevier.com/locate/conengprac

Input–output feedback linearizing control of linear induction motor taking into consideration the end-effects. Part I: Theoretical analysis

Francesco Alonge [a], Maurizio Cirrincione [b], Marcello Pucci [c,*], Antonino Sferlazza [a,c]

[a] D.E.I.M. (Department of Energy Information Engineering and Mathematical Models) of the National Research Council (CNR) of Italy, University of Palermo, Viale delle Scienze, 90128 Palermo, Italy
[b] The School of Engineering and Physics, The University of the South Pacific, Laucala Campus, Suva, Fiji Islands
[c] I.S.S.I.A. C.N.R. Section of Palermo (Institute on Intelligent Systems for Automation), via Dante 12, Palermo 90128, Italy

ARTICLE INFO

Article history:
Received 21 October 2013
Accepted 18 August 2014
Available online 5 December 2014

Keywords:
Linear induction motor (LIM)
Feedback linearization
End-effects

ABSTRACT

This first part of a paper, divided into two parts, deals with the theoretical formulation of the input–output feedback linearization (FL) control technique as to be applied to linear induction motors (LIMs). Linear induction motors, differently from rotating induction motors (RIMs), present other strong non-linearities caused by the so-called dynamic end effects, leading to a space-vector model with time-varying inductance and resistance terms and an additional braking force term. This paper, starting from a dynamic model of the LIM taking into consideration its dynamic end effects, previously developed by the same authors, defines a feedback linearization (FL) technique suited for LIMs, since it inherently considers its end effects. It further emphasizes the role of the LIM dynamic end effects in the LIM control formulation, highlighting the differences with respect to the corresponding technique for RIMs. It describes the control design criteria, taking also into consideration the constraints on the control and controlled variables, arising from the application of such control technique in a real scenario.

The second part of this paper describes the set of tests, both in numerical simulations and experiments, performed to assess the correctness of the proposed control technique.

1. Introduction

Linear induction motors (LIM) have been largely studied for several years (Boldea & Nasar, 1997, 1999; Laithwaite, 1975; Nasar & Boldea, 1987; Poloujadoff, 1980; Yamamura, 1979). Among the main reasons of their interest there is the opportunity to develop a direct linear motion without the need of any gear-box for the motion transformation (from rotating to linear). This advantage presents, as counterpart, the disadvantage of an increase of complexity of the machine model, presenting the so-called end effects and border effects. In particular, end effects are to be divided into two categories: (a) static and (b) dynamic end effects. Static end effects are due to asymmetries in the inductor structure in the longitudinal direction causing different reluctances of the magnetic paths of the three inductor phases. Dynamic end effects are caused by the relative motion between the short inductor and the induced part track and can be defined on the basis of the spatial representation, on the longitudinal direction of the LIM, of the root mean square (RMS) value of inductor MMF (magnetomotive force) profile. They are caused by the sudden growth of new currents in the induced part track. As a result, starting from the assumption that the rotating induction machine (RIM) presents a dynamic space-vector model which is non-linear (Leonhard, 2001; Vas, 1998), the dynamic model of the LIM presents further additional significant non-linearities, caused by the dynamic end effects.

The definition of a space-vector dynamic model of the LIM, taking into consideration the end effects, with a representation suitable for control purposes is not an easy task. Gentile, Rotondale, and Scarano (1987, 1988) propose a complete dynamic model of the LIM, taking into consideration both the static and dynamic end effects. It is, however, not adoptable for control purposes because of its complexity and strong dependence on the constructional aspects of the machine (pole pitch, air-gap length, thickness of the induced part track, slots width and depth, number of turns for phases etc.). Recently, a space-vector dynamic model of the LIM taking into consideration its dynamic end effects (not the static ones) has been developed and experimentally validated (Pucci, 2014). This last model has been expressed in a state-space form and is therefore particularly suitable for control purposes, in particular for the definition of state estimators, observers or novel control techniques taking into consideration the additional non-linearities arising from the presence of the dynamic end effects. If the space-vector state

* Corresponding author.
E-mail addresses: francesco.alonge@unipa.it (F. Alonge), m.cirrincione@ieee.org (M. Cirrincione), pucci@pa.issia.cnr.it (M. Pucci), antonino.sferlazza@unipa.it, sferlazza@pa.issia.cnr.it (A. Sferlazza).

http://dx.doi.org/10.1016/j.conengprac.2014.08.009
0967-0661/

List of symbols

u_{sx}, u_{sy}	inductor voltages in the induced part flux reference frame
i_{sx}, i_{sy}	inductor currents in the induced part flux reference frame
ψ_{rx}, ψ_{ry}	induced part fluxes in the induced part flux reference frame
F_e	electromagnetic thrust
F_r	load force
F_{eb}	braking force
$L_s(L_r)$	inductor (induced part) inductance
L_m	3-phase magnetizing inductance
$R_s(R_r)$	inductor (induced part) resistance
T_r	induced part time constant
σ	total leakage factor
ω_r	electrical angular speed of the induced part
ω_{mr}	electrical angular speed of the induced part flux
v	mechanical linear speed
a	mechanical linear acceleration
p	pole-pairs
τ_p	pole-pitch
τ_m	inductor length
M	inductor mass

model of the LIM in Pucci (2014) is considered, the additional strong non-linearities caused by the dynamic end effects are twofold:

(1) the presence of electric parameters of the model (inductances and resistance), which vary non-linearly with the machine speed;
(2) the presence of a braking force, whose terms depend on the square of induced part flux amplitude as well as on the product between the induced part flux amplitude and the inductor current components.

Although the LIM presents a far more non-linear model than the RIM, the approach adopted in the literature for its control has been usually to straightforwardly extend the classic control technologies developed for RIMs to LIMs.

The control system theory, however, offers an important corpus (Isidori, 1995; Khalil, 2002; Slotine & Li, 1991) of non-linear control methodologies for dealing with highly non-linear system. Among all, one of the most promising is the so-called input–output feedback linearization. Nevertheless, very few applications of non-linear control methods to electrical drives are provided by the scientific literature. Among these few applications, a very limited number of papers deal with the input–output feedback linearization of linear induction motors (Huang & Fu, 2003; Lin & Wai, 2001, 2002; Wai & Chu, 2007). All these papers approach the FL control of the LIM, adopting for the controller synthesis a dynamic model of the LIM which neglects both the static and the dynamic end effects. This corresponds to adopt the dynamic model of the equivalent rotating induction machine (RIM). From the controller design point of view, therefore, Lin and Wai (2001, 2002), Huang and Fu (2003), and Wai and Chu (2007) present exactly the same approach of Krzeminski et al. (1987), De Luca and Ulivi (1989), Kim, Ha, and Ko (1990), and Marino, Peresada, and Valigi (1993, 2010), which specifically propose the application of FL to RIM control. On the basis of the above, the state-of-the-art of the application of FL to LIMs corresponds to the state-of-the-art of the applications of FL to RIMs. For this reason, the main contributions of application of FL to RIMs should be briefly highlighted in the following. In particular, De Luca and Ulivi (1989) present an approach to the control of induction motors based on differential-geometric concepts, while, Marino et al. (1993) present a nonlinear adaptive state feedback input–output linearizing control. The current state-of-the-art is described by Marino et al. (2010).

This paper proposes an input–output feedback linearization (FL) technique for linear induction motors. The methodology is inspired from Marino et al. (2010), just as theoretical framework. The starting point of the proposed FL technique is, however, the space-vector dynamic model of the LIM taking into consideration its dynamic end effects recently developed by Pucci (2014). This model is particularly suitable for the application of the FL technique, since it is expressed in a state form. Starting from this dynamic space-vector model, a control system has been designed which, on the basis of the estimated induced part flux linkage and measured linear speed, outputs two suitably defined additional control variables. The control system is designed in such a way that the adoption of these control variables corresponds to deal with an equivalent LIM model which is linear and expressed in canonical control form. Finally, the real control variables of the machine, corresponding to the direct and quadrature components of the inductor voltages expressed in the inductor reference frame, are obtained from the additional ones after a set of suitably defined non-linear functions, depending on both these additional control inputs and the LIM electric variables (inductor currents, induced part flux linkage).

The proposed FL approach is thus able to take into consideration, besides the classic non-linearities of the RIM, even the further non-linearities caused by the dynamic end effects.

This paper is divided into two parts. The first part deals with the theoretical formulation of the input–output feedback linearization control technique as to be applied to linear induction motors. The second part describes the set of tests, both in numerical simulation and experimental, performed to assess the correctness of the control technique, and to verify the related dynamic performance.

2. Space-vector equivalent circuit of the LIM including end effects (Pucci, 2014)

In a LIM, differently from a RIM, the secondary (induced part), consists of a sheet of aluminum with a back core of iron. During the motion of the inductor, a continuous variation of the aluminum sheet happens, while the inductor presents a limited length. This causes a variation of the induced currents in the sheet and corresponding magnetic flux density in the air-gap, in proximity to the entrance (front of the motion) and exit (back of the motion) of the inductor. The amounts and signs of the flux modifications at the two ending parts of the inductor, meaning its entrance (in the direction of the motion) and its end (terminal part of the inductor in the direction of the motion), are different. When the moving inductor faces a new part of aluminum sheet, new induced currents are generated starting from a null value. The induced current, suddenly growing in a region of the induced part track where there was not insisting any magnetic flux, for the Faraday law arises trying to oppose to the magnetic flux increase. The effect is a deep reduction of the resulting flux in proximity to the entrance. At the same time, at the exit the induced current opposes to a sudden flux reduction from the inducer, creating an overall flux increase. The higher the speed of the inductor, the higher the end effect phenomenon. This last has been taken into consideration in the literature by the so-called end effect factor Q (da Silva, dos Santos, Machado, & De Oliveira, 2003; Duncan, 1983),

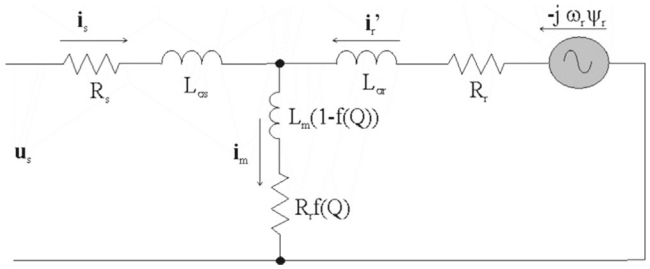

Fig. 1. Space-vector equivalent circuits of the LIM.

defined as

$$Q=\frac{\tau_m}{T_r v} \tag{1}$$

For the symbols, see the list at the beginning of the paper.

It can be observed that, the higher the machine speed, the higher the air-gap thickness (higher leakage inductance) and the lower the inductor length, the lower the factor Q. It means that the end effects increase with the machine speed, with the air-gap thickness and reduces with the inductor length.

Correspondingly, the three-phase magnetizing inductance varies with Q in the following way:

$$\hat{L}_m = L_m(1-f(Q)) \tag{2}$$

with:

$$f(Q)=\frac{1-e^{-Q}}{Q} \tag{3}$$

expressing the concept that the inductance virtually reduces with the end effects.

A computation of the overall losses of the machine shows that a resistance appears in the transversal branch taking into consideration the eddy current joule losses. This resistance is equal to:

$$\hat{R}_r = R_r f(Q) \tag{4}$$

Correspondingly, the space-vector equivalent circuit of the LIM can be deduced, as shown in Fig. 1. It could be observed that the main differences with the equivalent circuit of the RIM are in the magnetizing inductance and in the eddy current resistance (not to be confused with the resistance taking into consideration the magnetic losses of the machine), both present in the transversal branch (Pucci, 2014).

3. Space-vector model and field oriented control of the LIM

To the aim of describing the proposal FL technique, the space-vector dynamic model of the LIM, taking into consideration its dynamic end effects (Pucci, 2014), is written in the induced part flux reference frame, rotating at the angular speed ω_{mr}, as follows:

$$\frac{d\boldsymbol{i}_s}{dt}=-\gamma\boldsymbol{i}_s-j\omega_{mr}\boldsymbol{i}_s+\alpha\beta\boldsymbol{\psi}_r-j\beta\frac{p\pi}{\tau_p}v\boldsymbol{\psi}_r+\frac{\boldsymbol{u}_s}{\hat{\sigma}\hat{L}_s} \tag{5}$$

$$\frac{d\boldsymbol{\psi}_r}{dt}=-(\alpha-\eta)\boldsymbol{\psi}_r+\alpha\hat{L}_m\boldsymbol{i}_s-j\left(\omega_{mr}-\frac{p\pi}{\tau_p}v\right)\boldsymbol{\psi}_r \tag{6}$$

$$\frac{dv}{dt}=\mu(\boldsymbol{\psi}_r\wedge\boldsymbol{i}_s)-\frac{F_r}{M}-\frac{F_{eb}}{M} \tag{7}$$

$$F_{eb}=\vartheta\left[|\boldsymbol{\psi}_r|^2+L_{\sigma r}^2|\boldsymbol{i}_s|^2+L_{\sigma r}(\boldsymbol{\psi}_r\times\boldsymbol{i}_s)\right] \tag{8}$$

where " $\wedge$ " is the vector product, " $\times$ " is the scalar product and the variables α, β, γ, η, μ and ϑ are defined as follows:

$$\gamma=\frac{1}{\hat{\sigma}\hat{L}_s}\left[R_s+\hat{R}_r\left(1-\frac{\hat{L}_m}{\hat{L}_r}\right)+\frac{\hat{L}_m}{\hat{L}_r}\left(\frac{\hat{L}_m}{\hat{T}_r}-\hat{R}_r\right)\right];$$

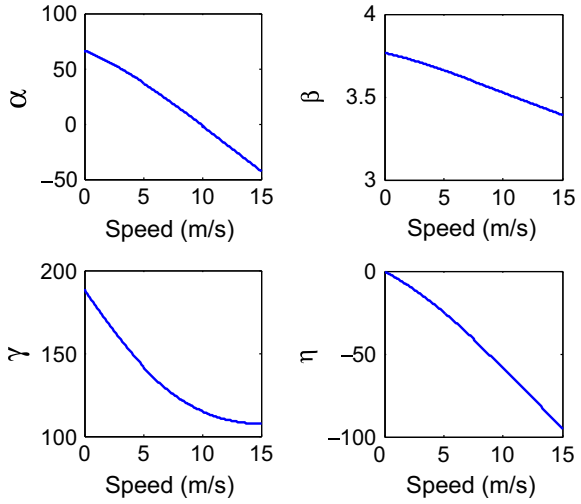

Fig. 2. Waveforms of α, β, γ and η.

$$\alpha=\left(\frac{1}{\hat{T}_r}-\frac{\hat{R}_r}{\hat{L}_m}\right);\quad \beta=\frac{\hat{L}_m}{\hat{\sigma}\hat{L}_s\hat{L}_r};\quad \eta=-\frac{\hat{R}_r}{\hat{L}_m};$$

$$\mu=\frac{3}{2}p\frac{\pi}{\tau_p}\frac{\hat{L}_m}{\hat{L}_r}\frac{1}{M};\quad \vartheta=\text{sign}(v)\frac{3}{2}\frac{L_r}{\hat{L}_r^2}\frac{1-e^{-Q}}{p\tau_p}$$

where

$$\hat{L}_m=L_m(1-f(Q));\quad \hat{L}_s=L_{\sigma s}+L_m(1-f(Q));$$
$$\hat{L}_r=L_{\sigma r}+L_m(1-f(Q));\quad \hat{R}_r=R_r f(Q);$$
$$\hat{T}_r=\frac{L_{\sigma r}+L_m(1-f(Q))}{R_r(1-f(Q))};\quad \hat{\sigma}=1-\frac{\hat{L}_m^2}{\hat{L}_r\hat{L}_s}.$$

These modified electrical parameters of the LIM have a precise physical meaning, as explained in Pucci (2014). In Fig. 2 the waveforms of α, β, γ and η are showed for the machine under test in a speed range varying between 0 and 15 m/s.

In the following the feedback linearization procedure based on the above model of LIM will be shown. The adopted linearization approach is the same as in Marino et al. (2010) where it has been developed and applied to the RIM. Here, however, some intriguing mathematical issues arising from the suitable definition of the dynamic end effects, will be focused. This will lead to the definition of additional control terms with respect to the RIM case, due to the dynamic end effects. In fact, differently from RIM case, the coefficients α, β, γ, η and μ are speed depending and thus time-variant parameters. This will lead to different feedback laws and further interesting consideration compared with the RIM model.

In order to obtain the feedback law for decoupling the dynamics of flux and velocity, it is useful writing the above-described model in terms of the space-vector direct and in-quadrature components:

$$\frac{di_{sx}}{dt}=-\gamma i_{sx}+\omega_{mr}i_{sy}+\alpha\beta\psi_{rx}+\beta\frac{p\pi}{\tau_p}v\psi_{ry}+\frac{u_{sx}}{\hat{\sigma}\hat{L}_s} \tag{9}$$

$$\frac{di_{sy}}{dt}=-\gamma i_{sy}-\omega_{mr}i_{sx}+\alpha\beta\psi_{ry}-\beta\frac{p\pi}{\tau_p}v\psi_{rx}+\frac{u_{sy}}{\hat{\sigma}\hat{L}_s} \tag{10}$$

$$\frac{d\psi_{rx}}{dt}=-(\alpha-\eta)\psi_{rx}+\alpha\hat{L}_m i_{sx}+\left(\omega_{mr}-\frac{p\pi}{\tau_p}v\right)\psi_{ry} \tag{11}$$

$$\frac{d\psi_{ry}}{dt}=-(\alpha-\eta)\psi_{ry}+\alpha\hat{L}_m i_{sy}-\left(\omega_{mr}-\frac{p\pi}{\tau_p}v\right)\psi_{rx} \tag{12}$$

$$\frac{dv}{dt}=\mu(\psi_{rx}i_{sy}-\psi_{ry}i_{sx})-\frac{F_r}{M}-\frac{F_{eb}}{M} \tag{13}$$

$$F_{eb}=\vartheta\left[(\psi_{rx}^2+\psi_{ry}^2)+L_{\sigma r}^2(i_{sx}^2+i_{sy}^2)+L_{\sigma r}(\psi_{rx}i_{sx}+\psi_{ry}i_{sx})\right] \tag{14}$$

In general, the rotating speed of the reference frame ω_{mr} can be chosen suitably. Indeed, if $\omega_{mr}=p\pi/\tau_p v+\alpha\hat{L}_m i_{sy}/\psi_{rx}$, Eq. (12) become $d\psi_{ry}/dt=-(\alpha-\eta)\psi_{ry}$. This implies that the flux component ψ_{ry} tends to zero exponentially with a variable time constant equal to $\hat{T}_r$. Moreover if the initial condition is $\psi_{ry}(0)=0$, then $\psi_{ry}(t)=0\ \forall t>0$.

The dynamic of the reference frame angle ρ_r can be written as $d\rho_r/dt=\omega_{mr}=p\pi/\tau_p v+\alpha\hat{L}_m i_{sy}/\psi_{rx}$.

With the above choices of ω_{mr} and $\psi_{ry}(0)=0$, it is ensured that the in-quadrature flux component is always null (these two choices from the physical point of view, can be obtained taking ω_{mr} equal to the speed of rotation of the induced part flux, and at the initial instant the direct axis of the reference frame must coincide with the space-vector of flux). The model (9)–(14) becomes

$$\frac{di_{sx}}{dt}=-\gamma i_{sx}+\frac{p\pi}{\tau_p}v i_{sy}+\frac{\alpha\hat{L}_m i_{sy}^2}{\psi_r}+\beta\alpha\psi_r+\frac{u_{sx}}{\hat{\sigma}\hat{L}_s} \tag{15}$$

$$\frac{di_{sy}}{dt}=-\gamma i_{sy}-\frac{p\pi}{\tau_p}v i_{sx}-\frac{\alpha\hat{L}_m i_{sy}i_{sx}}{\psi_r}-\beta\frac{p\pi}{\tau_p}v\psi_r+\frac{u_{sy}}{\hat{\sigma}\hat{L}_s} \tag{16}$$

$$\frac{d\psi_r}{dt}=-(\alpha-\eta)\psi_r+\alpha\hat{L}_m i_{sx} \tag{17}$$

$$\frac{d\rho}{dt}=\frac{p\pi}{\tau_p}v+\frac{\alpha\hat{L}_m i_{sy}}{|\psi_r|} \tag{18}$$

$$\frac{dv}{dt}=\mu(\psi_r i_{sy})-\frac{F_r}{M}-\frac{F_{eb}}{M} \tag{19}$$

$$F_{eb}=\vartheta\left[\psi_r^2+L_{\sigma r}^2(i_{sx}^2+i_{sy}^2)+L_{\sigma r}(\psi_r i_{sx})\right] \tag{20}$$

where $\psi_r=\psi_{rx}$.

Now, the two control inputs u_{sx} and u_{sy} are designed through a state feedback as follows:

$$u_{sx}=\hat{\sigma}\hat{L}_s\left[-\frac{p\pi}{\tau_p}v i_{sy}-\frac{\alpha\hat{L}_m i_{sy}^2}{|\psi_r|}-\beta\alpha\psi_r+\nu_x\right] \tag{21}$$

$$u_{sy}=\hat{\sigma}\hat{L}_s\left[+\frac{p\pi}{\tau_p}v i_{sx}+\frac{\alpha\hat{L}_m i_{sy}i_{sx}}{|\psi_r|}+\beta\frac{p\pi}{\tau_p}v\psi_r+\nu_y\right] \tag{22}$$

where ν_x and ν_y are additional control inputs that will be designed suitably. Replacing (21) and (22) in the model (15)–(20), the following equations are obtained:

$$\frac{di_{sx}}{dt}=-\gamma i_{sx}+\nu_x \tag{23}$$

$$\frac{di_{sy}}{dt}=-\gamma i_{sy}+\nu_y \tag{24}$$

$$\frac{d\psi_r}{dt}=-(\alpha-\eta)\psi_r+\alpha\hat{L}_m i_{sx} \tag{25}$$

$$\frac{d\rho}{dt}=\frac{p\pi}{\tau_p}v+\frac{\alpha\hat{L}_m i_{sy}}{|\psi_r|} \tag{26}$$

$$\frac{dv}{dt}=\mu(\psi_r i_{sy})-\frac{F_r}{M}-\frac{F_{eb}}{M} \tag{27}$$

$$F_{eb}=\vartheta\left[\psi_r^2+L_{\sigma r}^2(i_{sx}^2+i_{sy}^2)+L_{\sigma r}(\psi_r i_{sx})\right] \tag{28}$$

The model (23)–(28) is the basis of the field oriented control of the LIM taking into consideration the end effects (Pucci, 2012). Indeed with the feedback laws (21)–(22) and the suitably choice of ω_{mr} the dynamics of the inductor currents are made linear and decoupled between each other (a variation of ν_x produces only a variation of i_{sx}, and a variation of ν_y produces only a variation of i_{sy}). Moreover the flux depends only on i_{sx} and if the machine works at constant flux the thrust and thus the speed depends only on i_{sy}.

The end effects, besides modifying the decoupling laws (21)–(22), with respect to the RIM, add an additional term of braking force F_{eb}. As can be easily see from (28), a braking force $\vartheta\left[\psi_r^2+L_{\sigma r}^2 i_{sx}^2+L_{\sigma r}(\psi_r i_{sx})\right]$ is present varying with the flux level which is not present in the RIM model. Furthermore an addition of term $\vartheta L_{\sigma r}^2 i_{sy}^2$ appears that makes the speed dynamic nonlinear with respect to the input i_{sy}. This is an important difference between RIM and LIM: in the RIM the speed dynamic is linear with respect to i_{sy}, while in the LIM an additional nonlinear term $\vartheta L_{\sigma r}^2 i_{sy}^2$ appears. In the literature this nonlinear term has not yet been considered in other works, to the best of the authors' knowledge.

Remark 1. Feedback laws (21)–(22) hold only if $\psi_r\neq 0$, otherwise $\{u_{sx},u_{sy}\}\to\infty$ when $\psi_r\to 0$. This is a common feature with the RIM, where one existence condition for the linearizability of the model is that the flux amplitude was different from zero, in order to ensure that (21) and (22) were a diffeomorphism, i.e. it is an invertible function that maps one differentiable manifold to another, such that both the function and its inverse are smooth.

4. Input–output feedback linearization

As can be seen from model (23)–(28), the speed and flux dynamics are not decoupled in each working condition. Indeed the decoupling between speed and flux is valid only if the machine works at constant flux and the speed dynamic presents a nonlinearity with respect to the input. To overcome this problem, and to obtain a fully decoupled linear model, a further state feedback loop is deduced.

Let us define a new state variable a called *linear acceleration*, differently from i_{sy}:

$$a=\mu(\psi_r i_{sy})-\frac{F_r}{M}-\frac{F_{eb}}{M} \tag{29}$$

$$\begin{aligned}\frac{da}{dt}=&\frac{d\mu}{dt}\psi_r i_{sy}+\mu\frac{d\psi_r}{dt}i_{sy}+\mu\psi_r\frac{di_{sy}}{dt}+\frac{1}{M}\frac{d\vartheta}{dt}\left[\psi_r^2+L_{\sigma r}^2(i_{sx}^2+i_{sy}^2)+L_{\sigma r}(\psi_r i_{sx})\right]\\&+\frac{3}{2}\frac{L_r}{\hat{L}_r^2}\frac{(1-e^{-Q})}{p\tau_p M}\left[2\psi_r\frac{d\psi_r}{dt}+2L_{\sigma r}^2\left(i_{sx}\frac{i_{sx}}{dt}+i_{sy}\frac{i_{sy}}{dt}\right)\right.\\&\left.+L_{\sigma r}\left(\frac{\psi_r}{dt}i_{sx}+\psi_r\frac{i_{sx}}{dt}\right)\right]\end{aligned} \tag{30}$$

$$\begin{aligned}\frac{da}{dt}=&\frac{d\mu}{dt}\psi_r i_{sy}+\mu\frac{d\psi_r}{dt}i_{sy}+\mu\psi_r\frac{di_{sy}}{dt}+\frac{1}{M}\frac{d\vartheta}{dt}\left[\psi_r^2+L_{\sigma r}^2 i_{sy}^2\right]\\&+\frac{3}{2}\frac{L_r}{\hat{L}_r^2}\frac{(1-e^{-Q})}{p\tau_p M}\left[2\psi_r\frac{d\psi_r}{dt}+2L_{\sigma r}^2 i_{sy}\frac{i_{sy}}{dt}\right]\\=&[q_1-\mu(\alpha-\eta)]\psi_r i_{sy}+\mu\alpha\hat{L}_m i_{sx}i_{sy}-\gamma\mu\psi_r i_{sy}\\&+\left[q_2-2\frac{\vartheta}{M}(\alpha-\eta)\right]\psi_r^2+\frac{\alpha\vartheta}{M}\hat{L}_m i_{sx}+L_{\sigma r}^2\left(q_2-2\frac{\gamma\vartheta}{M}\right)i_{sy}^2\\&+\left(\mu\psi_r+2\frac{\vartheta}{M}L_{\sigma r}^2\right)\nu_y\end{aligned} \tag{31}$$

$$q_1 = \frac{d\mu}{dt} = \frac{3}{2} p \frac{\pi}{\tau_p} \frac{1}{M} \left[-\frac{L_{\sigma r} L_m}{\hat{L}_r^2} \frac{T_r a}{\tau_m} \left(1 - \left(1 + \frac{\tau_m}{T_r v} \right) e^{-\tau_m / T_r v} \right) \right] \tag{32}$$

$$q_2 = \frac{3}{2} \frac{L_r}{\hat{L}_r^2} \frac{1}{p \tau_p M} \frac{a}{v} \left[\frac{L_m}{\hat{L}_r^2} (1 - e^{-Q})(f(Q) - e^{-Q})(\hat{L}_r - L_m f(Q)) - Q e^{-Q} \right] \tag{33}$$

$$\nu_y = \frac{1}{\mu \psi_r + 2 \frac{\vartheta}{M} L_{\sigma r}^2} \left\{ -[q_1 - \mu(\alpha - \eta)] \psi_r i_{sy} - \mu \alpha \hat{L}_m i_{sx} i_{sy} + \gamma \mu \psi_r i_{sy} - \left[q_2 - 2 \frac{\vartheta}{M} (\alpha - \eta) \right] \psi_r^2 - \frac{\alpha \vartheta}{M} \hat{L}_m i_{sx} + - L_{\sigma r}^2 \left(q_2 - 2 \frac{\gamma \vartheta}{M} \right) i_{sy}^2 + \nu_{y'} \right\} \tag{34}$$

If the load thrust variation is assumed to be sufficiently slow, i.e. $\dot{F}_r \approx 0$, then the derivate of a can be written as in (30).

As can be seen from (30) both derivative of i_{sx} and derivative of i_{sy} are contained in (30). If (23) and (24) are replaced in (30) in order to compute the derivative of the acceleration, both the input ν_x and ν_y appear in the expression. Then *the model in this form cannot be feedback linearizable since the dynamic of speed cannot be made independent from* i_{sx}. This difficulty can be, in a first instance, overcome by exploiting a slight approximation which, however does not affect the correctness of the approach. The expression of F_{eb} in (28) is characterized by four terms. The terms $L_{\sigma r}^2 i_{sx}^2$ and $L_{\sigma r}(\psi_r i_{sx})$ due to the leakage induced part flux, could be reasonably neglected with respect to the term ψ_r^2 related to the main induced part flux, since $L_r^2 \gg L_{\sigma r}^2$. The expression of the braking thrust can be approximated as follows:

$$\tilde{F}_{eb} = \vartheta \left[\psi_r^2 + L_{\sigma r}^2 i_{sy}^2 \right] \tag{35}$$

Note that the braking effects due to the main flux is considered and only the effects due to the leakage induced part flux are neglected. Moreover the very important effect, presents only in the LIM model, of the nonlinearity of the speed dynamic with respect to the input represented by the term with i_{sy}^2 is considered with this approach. It should be noted that this term increases nonlinearly with quadratic law with the load force applied to the machine.

Remark 2. Here the consideration that the model cannot be feedback linearizable is evident from Eq. (30), however this can be proved with a rigorous mathematical formalism on the basis of the approach in Isidori (1995) and Khalil (2002), where the conditions, linked with the involutivity of the adjoint maps, making the considered model feedback linearizable, are provided.

Using the approximation (35), (30) can be replaced by (31), where q_1 and q_2 are defined in (32) and (33).

Remark 3. Note that q_1 and q_2 in (32) and (33) are a consequence of the end-effects and they are different from zero only during the acceleration and deceleration instants, that is when parameters vary because of the speed variation. During the steady-state $d\mu/dt = 0$ and $d\vartheta/dt = 0$, consequently $q_1 = q_2 = 0$. Fig. 3 shows the surfaces of q_1 and q_2 depending on the speed and acceleration for the machine under test (see Part II for details on the test set-up).

The feedback term that linearizes the speed dynamic can be defined as in (34).

Replacing (34) into (31) and writing the model (23)–(28) in terms of the new state variable (29) the following formulation can be obtained:

$$\frac{di_{sx}}{dt} = -\gamma i_{sx} + \nu_x \tag{36}$$

$$\frac{d\psi_r}{dt} = -(\alpha - \eta)\psi_r + \alpha \hat{L}_m i_{sx} \tag{37}$$

$$\frac{dv}{dt} = a \tag{38}$$

$$\frac{da}{dt} = \nu_{y'} \tag{39}$$

$$\frac{d\rho}{dt} = \frac{p\pi}{\tau_p} v + \frac{\alpha \hat{L}_m i_{sy}}{|\psi_r|} \tag{40}$$

$$q_3 = \frac{d(\alpha - \eta)}{dt} = \frac{R_r \hat{L}_r + R_r L_m (1 + f(Q))}{\hat{L}_r^2} \frac{T_r a}{\tau_m} \left[1 - \left(1 + \frac{\tau_m}{T_r v} \right) e^{-\tau_m / T_r v} \right] \tag{41}$$

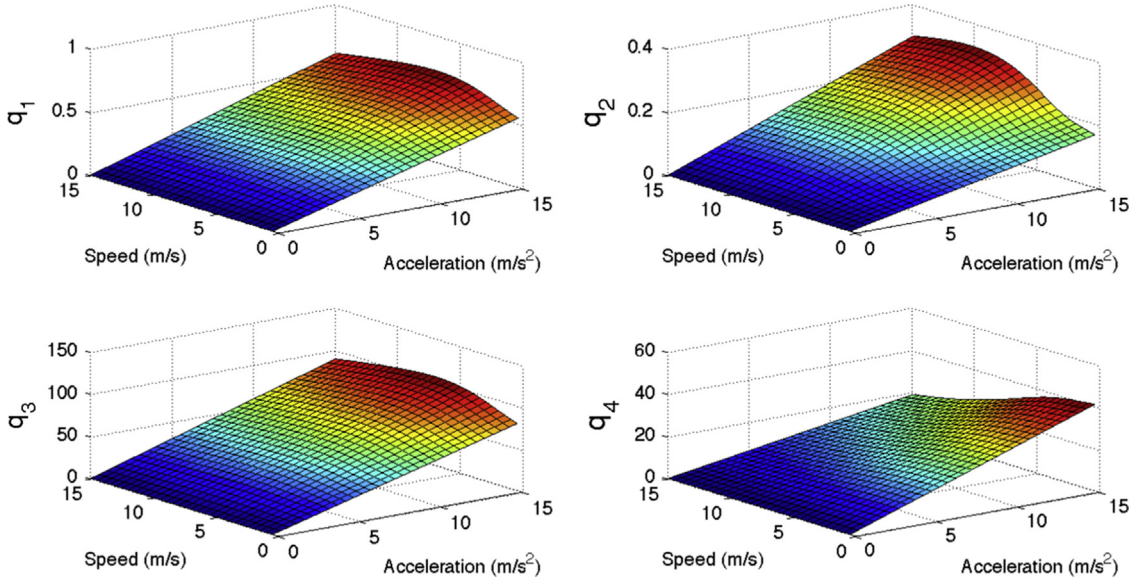

Fig. 3. Surfaces of q_1, q_2, q_3 and q_4 (whom analytic expressions are given respectively in (32), (33), (41) and (42) when the speed varies between 0 and 15 m/s and the acceleration varies between 0 and 15 m/s^2.

$$q_4 = \frac{d(\alpha\hat{L}_m)}{dt} = R_r\left[\frac{L_m^2}{\hat{L}_r^2}(1+f^2(Q))+1-2\frac{L_m f(Q)}{\hat{L}_r}\right]\frac{T_r a}{\tau_m}\left[1-\left(1+\frac{\tau_m}{T_r v}\right)e^{-\tau_m/T_r v}\right] \tag{42}$$

Now the flux and speed dynamic appear to be linear and decoupled and can be controlled through the inputs ν_x and ν_y'. Indeed speed does not depend from the flux transient even during flux variations. Finally the last step to linearize the model of the motor is the following. Let us introduce new state variable given by

$$\nu_\psi = -(\alpha-\eta)\psi_r + \alpha\hat{L}_m i_{sx} \tag{43}$$

Using (43) the time derivative of flux is $d\psi_r/dt = \nu_\psi$, and choosing as state variable ν_ψ instead of i_{sx} results:

$$\begin{aligned}\frac{d\nu_\psi}{dt} &= -\frac{d(\alpha-\eta)}{dt}\psi_r - (\alpha-\eta)\frac{d\psi_r}{dt} + \frac{d(\alpha\hat{L}_m)}{dt}i_{sx} + \alpha\hat{L}_m\frac{di_{sx}}{dt}\\ &= -q_3\psi_r - (\alpha-\eta)\left(-(\alpha-\eta)\psi_r + \alpha\hat{L}_m i_{sx}\right)\\ &\quad + q_4 i_{sx} + \alpha\hat{L}_m(-\gamma i_{sx} + \nu_x)\end{aligned} \tag{44}$$

where q_3 and q_4 are defined in (41) and (42). For (41) and (42) the same comment given in Remark 3 for (32) and (33) is valid. Fig. 3 shows the surfaces of q_3 and q_4 depending on the speed and acceleration.

Let define also:

$$\nu_x = \frac{q_3\psi_r}{\alpha\hat{L}_m} - \frac{(\alpha-\eta)^2}{\alpha\hat{L}_m}\psi_r + (\alpha-\eta)i_{sx} - \frac{q_3 i_{sx}}{\alpha\hat{L}_m} + \gamma i_{sx} + \frac{\nu_x'}{\alpha\hat{L}_m} \tag{45}$$

such that the model (36)–(40) can be finally written as

$$\frac{d\psi_r}{dt} = \nu_\psi \tag{46}$$

$$\frac{d\nu_\psi}{dt} = \nu_x' \tag{47}$$

$$\frac{dv}{dt} = a \tag{48}$$

$$\frac{da}{dt} = \nu_y' \tag{49}$$

This model (46)–(49) is the linearized model of the linear induction motor with decoupled speed and flux dynamics.

In summary to achieve the input–output feedback linearizing control of LIM, considering the end effects, the inputs ν_x' and ν_y' have to be chosen to fix the flux and speed dynamic of the model (46)–(49). Then through a first state feedback ν_x and ν_y are obtained starting from ν_x' and ν_y' by (34) and (45). Finally through a second state feedback given by (21) and (22) the voltage source u_{sx} and u_{sy} are obtained starting from ν_x and ν_y. Note that the only condition to ensure the existence of this feedback is that the flux $|\psi_r|$ is different from zero (see Remark 1), while the feedback given by (45) and (34) always exist for any working condition. This constraint is coherent with the physical constraint that the machine can correctly work only if magnetized.

5. Controller design

In order to make ψ_r and v track their references ψ_{ref} and v_{ref}, the input signals ν_x' and ν_y' are designed as

$$\nu_x' = -k_{\psi 1}\left(\psi_r - \psi_{ref}\right) - k_{\psi 2}\left(\nu_\psi - \frac{d\psi_{ref}}{dt}\right) + \frac{d^2\psi_{ref}}{dt^2} \tag{50}$$

$$\nu_y' = -k_{v1}\left(v - v_{ref}\right) - k_{v2}\left(a - \frac{dv_{ref}}{dt}\right) + \frac{d^2 v_{ref}}{dt^2} \tag{51}$$

where $k_{\psi 1}$, $k_{\psi 2}$, k_{v1} and k_{v2} are positive constant design parameters to be determined in order to impose an exponentially stable dynamic of the decoupled, linear, time-invariant, second order systems (52)–(53), constituted by the flux and speed errors $e_{\psi_r} = \psi_r - \psi_{ref}$ and $e_v = v - v_{ref}$.

$$\frac{d^2 e_{\psi_r}}{dt^2} = -k_{\psi 1}e_{\psi_r} - k_{\psi 2}\frac{de_{\psi_r}}{dt} \tag{52}$$

$$\frac{d^2 e_v}{dt^2} = -k_{v1}e_v - k_{v2}\frac{de_v}{dt} \tag{53}$$

In order to verify the improvements in the dynamic performance achievable with the adoption of the proposed FL control techniques, in Part II of this paper, it will be compared with the industrial standard in high performance control of induction motors: field oriented control (FOC). FOC has been implemented here in a improved form, so to take into consideration the LIM dynamic end effects (Pucci, 2012). In particular, in order to compare the feedback linearization control to the FOC, the parameters $k_{\psi 1}$, $k_{\psi 2}$, k_{v1} and k_{v2}, and the parameters of the PI in the FOC have to be chosen such that the two closed loop systems present the same closed loop dynamics. In this case, the same bandwidth and the same phase-margin of the closed loop system are imposed. Using the controllers tuned with the parameters given in Table 1, both for FOC and FL, the bode diagrams of the transfer functions of the closed loop systems, plotted in Figs. 4 and 5, are obtained. From these figures can be easily observed that the two systems, respectively LIM controlled with FL and LIM controlled with FOC, have the same bandwidths and the same phase margins, as reported in Table 2. However in order to obtain the transfer functions in the FOC case, the assumptions of constant parameters and constant flux amplitude have to be made. In particular, as for the transfer function of the flux, the parameters obtained at rated speed are considered, as for the transfer function of the speed, the parameters obtained at rated flux are considered.

Table 1
Parameters of the controllers.

FOC		FL
$K_{P,i_{sx}} = \frac{2}{3}250$	$K_{I,i_{sx}} = \frac{2}{3}10^5$	$k_{\psi 1} = 100,000$
$K_{P,i_{sy}} = \frac{2}{3}250$	$K_{I,i_{sy}} = \frac{2}{3}10^5$	$k_{\psi 2} = 200$
$K_{P,\psi_r} = 10$	$K_{I,\psi_r} = 30$	$k_{v1} = 10,000$
$K_{P,v} = 17$	$K_{I,v} = 8$	$k_{v2} = 300$

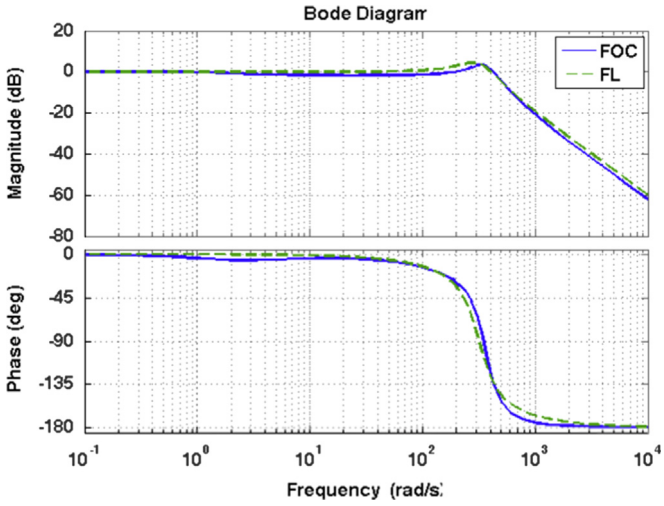

Fig. 4. Bode diagram of closed loop transfer function of the flux.

This control design is a limitation for the FOC compared with the FL: in the FL the specifics given in Table 2 are satisfied in all working conditions, while in the FOC these specifics could change if the flux and the speed are different from the rated one. They are thus rigorously respected under one only working condition. This fact is evident, because if the motor is controlled by FL the closed loop transfer function can be deduced from (52) and (53) where no physic parameters appear, while if the motor is controlled by FOC the closed loop transfer function contains the machine parameters that are varying with speed (due to the end effects) and flux.

5.1. System constraints

From a theoretical point of view, no physical constraints on the system are to be considered, however in real applications there are limits that have to be satisfied: the currents are to be limited in order to avoid the damage of the motor and the voltage limits introduced by the inverter are to be taken into consideration. With regard to the FOC, these problems can be easily solved directly by means of saturations at the output of PIs. If FL control is used, these problems have to be taken into consideration in an indirect way, limiting the control input ν_x' and ν_y'. In fact, by limiting ν_x' and ν_y', the currents i_{sx} and i_{sy} are indirectly limited. In particular, the inductor current i_{sx}, in FL, as can be easily seen from Eq. (43), is proportional to ν_ψ, so for a fixed value of ν_ψ, corresponds a value of i_{sx}:

$$i_{sx} = \frac{1}{\alpha \hat{L}_m}[\nu_\psi + (\alpha - \eta)\psi_r] \tag{54}$$

The equality (54) has been used here to fix the maximum current value, indirectly acting the maximum value of ν_ψ. However (54) needs the knowledge of flux and speed, so a constant maximum value of current corresponds to different values of ν_ψ depending on the working conditions. This is not problematic since the same knowledge of flux and speed is needed to compute the feedback laws, thus the same variables can be used to compute instantaneously the value of i_{sx}. With regard to inductor current term i_{sy}, the same consideration given for i_{sx} could be made, where the variable a is considered instead of ν_ψ. In this case the inputs are limited such that the maximum currents in both FL case and FOC case are the same.

Finally, in FL control there is another problem linked with the constraints that is not present in FOC. In fact the maximum current is not the only variable to be taken into consideration when the limits on the variables are chosen, but it is essential that the voltage given in input to the inverter is not bigger than the voltage that the inverter is able to generate; if the source voltage of the motor is smaller than the voltage given by the output of the feedback linearization process, the linearization cannot work. This fact is obvious because the current and flux needed in the linearization process are not coherent with the voltages produced from the linearization process itself.

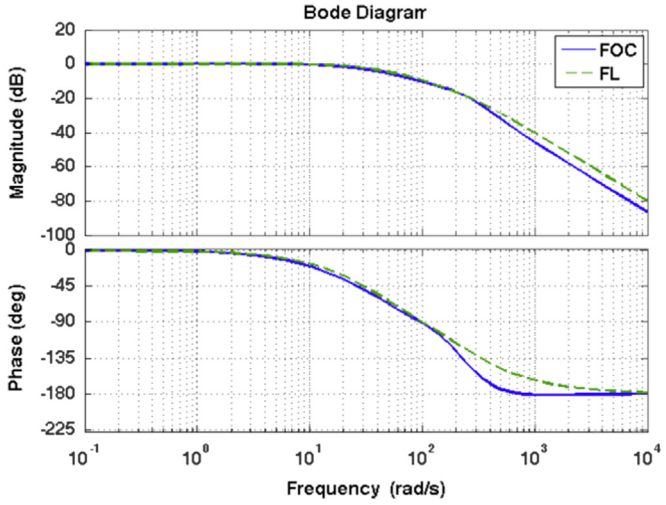

Fig. 5. Bode diagram of closed loop transfer function of the speed.

Table 2
Design specifics.

Control indeces	Speed	Flux
Bandwidth	$B_{-3db} = 37$ rad/s	$B_{-3db} = 455$ rad/s
Phase margin	$m_\phi = 128^\circ$	$m_\phi = 40^\circ$

6. Control scheme

The block diagram of the overall control scheme is drawn in Fig. 6.

The block "input–output FL" receives in input variables the reference and estimated induced part fluxes, the reference and measured linear speeds, the measured direct and quadrature current components i_{sx}, i_{sy} and provides in output the direct and quadrature components of the inductor voltages u_{sx}, u_{sy}. The coordinate transformation from and to the induced part flux reference frame is performed by vector rotations on the basis of the instantaneous knowledge of the induced part flux angle ρ_r. It should be noted that the angular position ρ_r, needed for the correct field orientation, is provided by the block "flux model". In this case, the "current model" based on the induced part equations

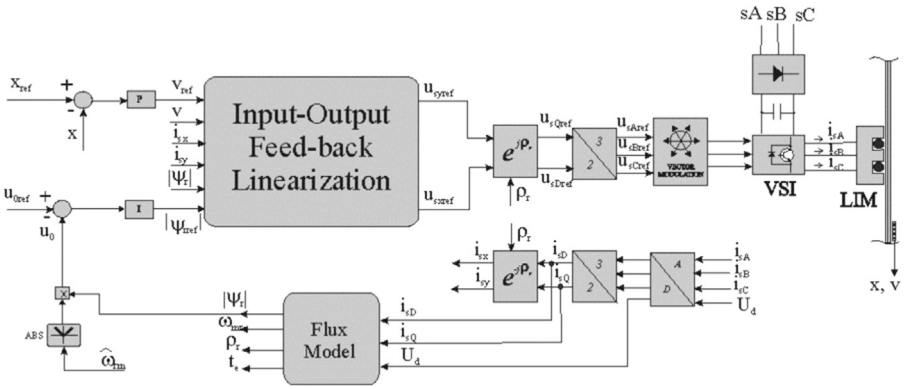

Fig. 6. Block diagram of the overall control scheme of the LIM drive based on the input–output FL.

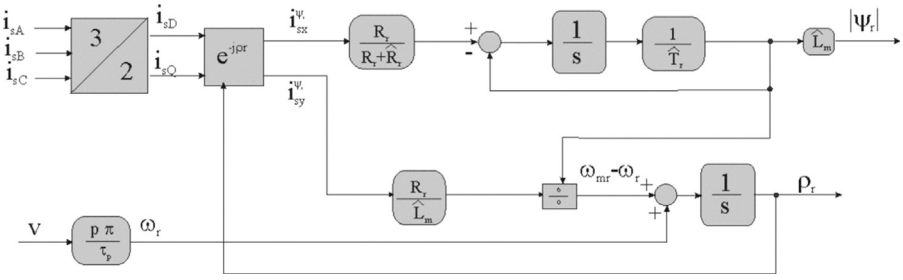

Fig. 7. Block diagram of the "current model" in the induced part flux reference frame.

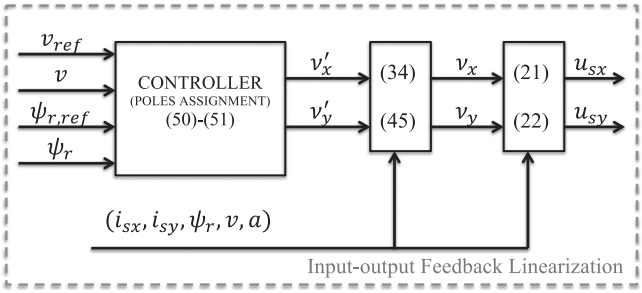

Fig. 8. Block diagram of the feedback control scheme.

written in the induced part flux reference frame, specifically developed for LIM and taking into consideration its end effects (Pucci, 2012), has been adopted because of its null sensitivity to the variation of the inductor resistance and because of its closed-loop integration feature. On the contrary, its significant sensitivity versus the variations of the induced part time constant is well known. With particular reference to phase estimation of the induced part flux space-vector, taking into consideration the end effects of the LIM is particularly important, since it guarantees the conditions of correct flux orientation and therefore maintains the full thrust capability of the drive. This flux model is described by the following equation:

$$\frac{d\boldsymbol{\psi}_r}{dt} = -\frac{1}{\hat{T}_r}\boldsymbol{\psi}_r + \left(\frac{\hat{L}_m}{\hat{T}_r} - \hat{R}_r\right)\boldsymbol{i}_s - j\left(\omega_{mr} - \frac{p\pi}{\tau_p}v\right)\boldsymbol{\psi}_r \tag{55}$$

The block diagram of (55) is shown in Fig. 7.

The block diagram of the feedback control scheme is represented in Fig. 8.

Furthermore, on the direct axis (x), a voltage control loop commands the flux loop to permit the drive to work automatically in the field weakening region by maintaining the product of the induced part flux amplitude and the absolute value of the angular electrical speed of the induced part constant. On the quadrature axis (y), the position loop controls the speed loop. If the position control loop is disabled, the LIM drive can work in speed control mode. The inductor voltage phase references are provided to a space-vector pulsewidth modulator (SV-PWM), which permits the inductor voltages to be properly synthesized. As far as both the numerical simulations and the experiments are concerned, in both the FL and FOC cases, a sampling frequency of 10 kHz and a PWM frequency of 5 kHz have been set.

7. Conclusion

This is the first part of a paper divided into two parts, dealing with the formulation and application of the input–output feedback linearization (FL) control technique to linear induction motors (LIM). It discusses the suitability of the adoption of the input–output FL control for LIMs, motivated by the presence of additional strong non-linearities with respect to the RIM case, leading to the presence of speed-varying machine parameters and braking force term. This paper, starting from a recently developed dynamic model of the LIM taking into consideration its end effects, defines the theoretical framework of the FL technique suited for LIMs, since it inherently considers its end effects. This part of the paper describes the design of the FL control system, obtained by the definition of suitable control variables permitting to deal with an equivalent LIM model which is linear and expressed in canonical control form. The set of non-linear transformations permitting to obtain the real LIM control variables on the basis of the additional ones is defined and shown in the paper. Correspondingly, the conditions under which the LIM model is feedback linearizable are defined. In particular, this part of the paper emphasizes the role of the LIM dynamic end effects in the LIM control formulation, highlighting the differences with respect to the corresponding technique for RIMs. It describes the control design criteria, taking also into consideration the constraints on the control and controlled variables, arising from the application of such control technique in a real scenario.

References

Boldea, I., & Nasar, S. A. (1997). *Linear motion electromagnetic devices*. New York, USA: Taylor & Francis.

Boldea, I., & Nasar, S. A. (1999). Linear electric actuators and generators. *IEEE Transactions on Energy Conversion*, *14*(3), 712–717.

da Silva, E. F., dos Santos, E. B., Machado, P., & De Oliveira, M. (2003). Dynamic model for linear induction motors. In *2003 IEEE International Conference on Industrial Technology, IEEE* (Vol. 1, pp. 478–482).

De Luca, A., & Ulivi, G. (1989). Design of an exact nonlinear controller for induction motors. *IEEE Transactions on Automatic Control*, *34*(12), 1304–1307.

Duncan, J. (1983). Linear induction motor-equivalent-circuit model. *IEE Proceedings B Electric Power Applications* (*IET*), *130*, 51–57.

Gentile, G., Rotondale, N., & Scarano, M. (1987). *Analisi del funzionamento transitorio del motore lineare* (5).

Gentile, G., Rotondale, N., & Scarano, M. (1988). *The linear induction motor in transient operation* (7–8).

Huang, C.-I., & Fu, L.-C. (2003). Passivity based control of the double inverted pendulum driven by a linear induction motor. In *Proceedings of 2003 IEEE conference on control applications, CCA 2003, IEEE* (Vol. 2, pp. 797–802).

Isidori, A. (1995). *Nonlinear control systems* (third edition). London, UK: Springer.

Khalil, H. K. (2002). *Nonlinear systems*, Vol. 3. Upper Saddle River: Prentice hall.

Kim, D.-I., Ha, I.-J., & Ko, M.-S. (1990). Control of induction motors via feedback linearization with input–output decoupling. *International Journal of Control*, *51*(4), 863–883.

Krzeminski, Z., et al. (1987). Nonlinear control of induction motor. In *10th IFAC World Congress* (Vol. 349, p. 33). Munich.

Laithwaite, E. R. (1975). Linear electric machines—personal view. *Proceedings of the IEEE*, *63*(2), 250–290.

Leonhard, W. (2001). *Control of electrical drives*. Berlin, Germany: Springer.

Lin, F.-J., & Wai, R.-J. (2001). Hybrid control using recurrent fuzzy neural network for linear induction motor servo drive. *IEEE Transactions on Fuzzy Systems*, *9*(1), 102–115.

Lin, F.-J., & Wai, R.-J. (2002). Robust control using neural network uncertainty observer for linear induction motor servo drive. *IEEE Transactions on Power Electronics*, *17*(2), 241–254.

Marino, R., Peresada, S., & Valigi, P. (1993). Adaptive input–output linearizing control of induction motors. *IEEE Transactions on Automatic Control*, *38*(2), 208–221.

Marino, R., Tomei, P., & Verrelli, C. M. (2010). *Induction motor control design*. London, UK: Springer.
Nasar, S. A., & Boldea, I. (1987). *Linear electric motors: Theory, design, and practical application*. New York, USA: Prentice-Hall Inc.
Poloujadoff, M. (1980). *The theory of linear induction machinery*. Oxford, UK: Clarendon Press.
Pucci, M. (2012). Direct field oriented control of linear induction motors. *Electric Power Systems Research*, *89*, 11–22.
Pucci, M. (2014). State space-vector model of linear induction motors. *IEEE Transactions on Industry Applications*, *50*(1), 195–207.
Slotine, J.-J. E., Li, W., et al. (1991). *Applied nonlinear control*, Vol. 199. New Jersey: Prentice Hall.
Vas, P. (1998). *Sensorless vector and direct torque control*. Oxford, UK: Oxford University Press.
Wai, R.-J., & Chu, C.-C. (2007). Robust petri fuzzy-neural-network control for linear induction motor drive. *IEEE Transactions on Industrial Electronics*, *54*(1), 177–189.
Yamamura, S. (1979). *Theory of linear induction motors* (Vol. 246, p. 1). New York: Halsted Press.